Polymer 49 (2008) 3399–3412

Contents lists available at ScienceDirect

Polymer

journal homepage: www.elsevier.com/locate/polymer

Crosslinking systems and film properties for surfactant-free latexes based on anhydride-containing polymers

Willem Jan Soer [a,b], Weihua Ming [a,c,*], Cor E. Koning [b,**], Rolf A.T.M. van Benthem [a]

[a] Laboratory of Materials and Interface Chemistry, Eindhoven University of Technology, P.O. Box 513, 5600 MB Eindhoven, The Netherlands
[b] Laboratory of Polymer Chemistry, Eindhoven University of Technology, P.O. Box 513, 5600 MB Eindhoven, The Netherlands
[c] Nanostructured Polymers Research Center, Materials Science Program, University of New Hampshire, Durham, NH 03824, USA

ARTICLE INFO

Article history:
Received 2 May 2008
Received in revised form 21 May 2008
Accepted 1 June 2008
Available online 7 June 2008

Keywords:
Artificial latex
Crosslinker
Film formation

ABSTRACT

In this paper, we report novel crosslinking systems for surfactant-free artificial latexes based on anhydride-containing polymers. Surfactant-free latexes with average particle diameters of about 150 nm and a ζ-potential of −70 mV have been successfully obtained from anhydride-containing polymers with various T_gs and polarities, including poly(octadecene-*alt*-maleic anhydride) (POMA) and maleinized polybutadiene (PBDMA). When adipic dihydrazide (ADH), a water-soluble crosslinker, was added to these latexes, no differences in particle size or ζ-potential were found; the presence of ADH did not affect the latex stability. In contrast, when 1,6-diaminohexane (DAH) was added to these latexes, it was found to interact with the polymer particles, indicated by a decrease in absolute ζ-potential for the latex particles and even gelation in the case of POMA. From ^{1}H NMR and LC–MS studies, it has been shown that no free DAH was present after being added to the latex, while free, unreacted ADH was present in aqueous phase upon its addition to the latex. Kinetic studies revealed that irreversible imide formation between anhydride and ADH took place at temperatures of 90 °C and above. In comparison, DAH only formed imides with the copolymers at significantly higher curing temperatures, i.e. >130 °C. Furthermore, the film formation of these latexes was studied; for the different copolymer latexes, curing at temperatures above the T_g of the respective copolymers led to homogeneous film formation. These systems based on surfactant-free latexes crosslinked with ADH have displayed promising properties for future coating applications.

1. Introduction

Because of increasing concerns on volatile organic compounds from polymer coatings, water-borne coatings have become increasingly important. Acrylic, alkyd, epoxy, polyurethane, polyester and other resins are widely used in the formulation of water-borne coatings [1,2] in the form of either synthesized latexes (primary dispersions) or artificial latexes (secondary dispersions). We have successfully prepared surfactant-free, artificial latexes from modified poly(styrene-*alt*-maleic anhydride) (PSMA), which are stabilized by electrostatic interactions [3]. Although PSMA displays some very interesting properties in relation to coating applications, such as being used as surfactant, the direct use of this polymer as a resin for coating applications is very limited [4]. One of the drawbacks of PSMA is its high T_g (175 °C for unmodified PSMA and 130 °C for the polymer used in this study [3]). Therefore, in this paper, two other anhydride-containing polymers with lower T_g will be studied, aiming at future coating applications. One is poly(octadecene-*alt*-maleic anhydride) (POMA, T_g = ~95 °C), and the other is maleinized polybutadiene (PBDMA, with 17 wt% maleic anhydride grafted onto polybutadiene; T_g of −70 °C). The approach that was used for the preparation of PSMA latexes as described elsewhere [3] should also allow the preparation of artificial latexes from POMA and PBDMA.

To obtain a protective coating with good resistance against organic solvents, a homogeneous and densely crosslinked network needs to be formed. Crosslinking of a latex can take place in three different ways, i.e. intraparticle (or core-crosslinked), interparticle (shell-crosslinked), or homogeneous crosslinking, as shown in Fig. 1. The shell-crosslinked and homogeneously crosslinked films are expected to give better mechanical properties than the core-crosslinked films, since the latter do not have a continuous crosslinked phase and, therewith, lack coherence [5]. Therefore, the film

* Corresponding author. Nanostructured Polymers Research Center, Materials Science Program, University of New Hampshire, 23 College Road, Durham, NH 03824, USA.
** Corresponding author.
E-mail addresses: w.ming@unh.edu (W. Ming), c.e.koning@tue.nl (C.E. Koning).

0032-3861/$ – see front matter © 2008 Elsevier Ltd. All rights reserved.
doi:10.1016/j.polymer.2008.06.002

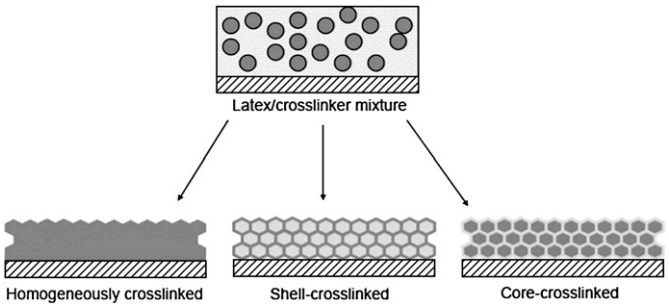

Fig. 1. Different crosslinking mechanisms where the dark parts represent the crosslinked material and the light parts represent the non-crosslinked material.

formation and interdiffusion of the crosslinker and the polymer must take place before the crosslinking is completed [6]; otherwise, inhomogeneously crosslinked film would be resulted.

Crosslinking of anhydride-containing polymers can be accomplished with multi-functional alcohols, but reaction times between anhydrides and alcohols, leading to half esters, are usually long. Furthermore, high temperatures are needed [7,8] at which the equilibrium will shift to the left, leading to low crosslinking efficiencies. Esters are also known to hydrolyze relatively easily, leading to poor water resistance. Therefore, alcohols are not effective crosslinkers for the anhydride-containing latexes studied in this work. Another class of crosslinker is aliphatic di- or polyamine [9], such as 1,6-diaminohexane (DAH), but apart from toxicity and a strong smell, high temperatures are required (>125 °C) to form irreversible imides [10]. Adipic dihydrazide (ADH), a water-soluble compound that lacks the toxicity and strong smell of primary amines, can be potentially used as a crosslinker. Crosslinking reactions between hydrazides and carbonyl moieties were described in literature [11–14], resulting in hydrazone groups [15]. Reactions between hydrazides and anhydrides were attempted at low application temperatures (<50 °C) [14,16], which would not ring-close to form imides and, therefore, lead to reversible bonds [10].

In this study, we aim at 1-K crosslinking systems (the crosslinker and the reactive latex in one package, without premature reaction), so the crosslinkers should not affect the latex stability and preferably be water soluble. Both ADH and DAH will be investigated as potential crosslinkers for anhydride-containing artificial latexes. Their interaction with latex particles and crosslinking reaction with latex polymers, as well as the film formation property of the latexes in the presence of the crosslinkers, will be examined.

2. Experimental

2.1. Materials

All materials were purchased from Aldrich and used as-received, unless noted otherwise. Solvents were purchased from Biosolve and used without further purification. Adipic dihydrazide (ADH) was kindly supplied by DSM NeoResins and used without purification. 1,6-Diaminohexane (DAH) was purchased from VWR. *cis*-1,2-Cyclohexyldicarboxylic anhydride (CDA) was purchased from Acros. Poly(styrene-*alt*-maleic anhydride) (PSMA; trademark: SMA1000F) and the ammonium salt thereof (SMA1000H) and maleinized polybutadiene (17 wt% maleic anhydride) (PBDMA; trademark: Ricon 131MA17) were kindly provided by Sartomer and used as-received. Poly(octadecene-*alt*-maleic anhydride) (POMA) was purchased from Aldrich. Deuterated solvents were obtained from Cambridge Isotope Laboratories, Inc.

2.2. Latex properties

The formation of PSMA-based latexes has been described elsewhere [3]. The latex used in this study consisted of PSMA with 30 mol% of the anhydride imidized with *n*-heptylamine. Another 30 mol% of the initial anhydride was ammonolyzed to obtain electrostatic stability. The remaining 40 mol% of anhydride was available for crosslinking. Latexes from POMA and PBDMA were obtained via the same process as previously described [3]; 50 mol% of the amount of the initial anhydride was ammonolyzed, without any further imidization. The concentrations of the dropwise-added solutions were varied to tune the particle diameters for different polymers.

2.3. Film formation

For AFM studies, 10 wt% latexes containing crosslinker (ADH or DAH) were drop-cast on glass substrates of $\sim 2 \times 2$ cm^2, and cured in an oven at elevated temperatures for 15 min. Films that were formed at temperatures of 100 °C or lower were cured for longer period of time, as indicated in the text, to ensure that water had been evaporated and the crosslinking was completed.

2.4. Characterization

Differential scanning calorimetry (DSC) was carried out on a Perkin–Elmer Pyris 1 differential scanning calorimeter. PSMA and POMA samples were heated from 20 to 180 °C at a rate of 10 °C/min followed by an isothermal period of 5 min. A cooling cycle to 25 °C at 10 °C/min was performed prior to a second heating run to 180 °C at 10 °C/min. PBDMA samples were cooled from 30 to −110 °C at 50 °C/min, followed by an isothermal period of 10 min. A heating step from −110 to 50 °C was performed at 20 °C/min followed by an isothermal period of 1 min. Second cooling and heating steps at 30 and 20 °C/min, respectively, were performed, with an isothermal period of 10 min at −110 °C. The T_g was determined from the second heating run.

^{1}H and ^{13}C NMR analyses were performed on a Varian Gemini 300 or Mercury 400 instrument, in deuterated DMSO, chloroform or water. The interaction between a crosslinker and a latex was studied by adding 1 ml of the latex to a solution of the respective crosslinker in deuterated water at room temperature. To quantify the amount of crosslinker that reacted with the latex particles, sodium 3-(trimethylsilyl)propionate-d_4 (TSP) was used as an internal standard [17], and added to the crosslinker solution in D_2O. To study the crosslink reaction mechanism, CDA was dissolved in DMSO-d_6 to which crosslinker, ADH or DAH, was dropwise added at 180 °C. Samples were taken at different intervals and cooled to room temperature, prior to the measurement. The final dried product was studied in deuterated chloroform.

Dynamic light scattering (DLS) and ζ-potential measurements were performed on a Malvern ZetaSizer Nano ZS at 20 °C. The particle size and its distribution thereof were determined according to ISO 13321 (1996). The solid content of the latex samples was ~0.1 wt%. The amounts of crosslinker, DAH or ADH, added to the latex were 30 mol% with respect to the initial anhydride present in the polymer. The pH dependence measurements of size and ζ-potential were performed by adding a 0.071 M HNO_3 or 0.1 M NaOH aqueous solution to the latex with a Malvern MPT-2 Autotitrator, starting at the pH of the latex as prepared. The pH value was stepwise altered in steps of 0.5 and left for 1 min at this pH prior to the next ζ-potential and particle size determination, until a pH value of 2 was reached or flocculation occurred in case of the acidic titration, or pH 12 was reached for the basic titration. The ζ-potential was calculated from the electrophoretic mobility (μ) using the Smoluchowski relationship, $\zeta = \eta\mu/\varepsilon$, where $\kappa a \gg 1$ (where η is

the solution viscosity, ε is the dielectric constant of the medium, and κ and a are the Debye–Hückel parameter and the particle radius, respectively).

Cryogenic-transmission electron microscopy (cryo-TEM) was performed on a FEI Tecnai G2 Sphera microscope at −170 °C, operated at 200 kV. Samples (3 μl) of 1 wt% latex were applied to a glow discharged Lacy grid in a Vitrobot™ (PC controlled vitrification robot, FEI) instrument at 22 °C and 100% relative humidity. The excess of latex was removed by blotting with a filter paper, followed by vitrification of the film by insertion into liquid ethane at −172 °C. Photos were obtained with a Gatan 1k × 1k CCD camera.

Attenuated total reflection Fourier transform infrared (ATR-FTIR) spectroscopy was performed on a Bio-Rad Excalibur FTS3000MX infrared spectrophotometer (4 scans per spectrum, resolution 4 cm^{-1}) with an ATR diamond unit (Golden Gate). The measurement was performed by mixing a DMSO solution of the material (or the latex) and a H_2O solution of crosslinker prior to applying the mixture on the ATR diamond. The ratio of theoretically present anhydride and hydrazide or amine functional groups from the crosslinker was kept at 1. A full spectrum was taken every 5, 10 or 20 s (depending on the reaction rate). Heights of the carbonyl peaks were taken as a measure of the extent of the reaction.

Atomic force microscopy (AFM) experiments on films were performed on a NT/MDT Solver P47HT, with a scanning rate of 0.2 Hz, in semi-contact mode under atmospheric conditions, using high resolution non-contact gold-coated silicon cantilevers from the NSG11 series (NTI-Europe) with spring constant $k = 2.5$–10 N/m and typical resonance frequency of 150 kHz.

3. Results and discussion

Artificial latexes from different polymers (Table 1) were prepared similar to the procedure as described previously [3]. The different polymers used in this study will lead to large differences in the final properties of the films. PBDMA-based latexes can form flexible films due to its low T_g, while POMA will give the final film with a hydrophobic character [18].

3.1. Preparation of anhydride-containing artificial latexes

3.1.1. Preparation and properties of PSMA-based latexes

The particle size of the latexes was influenced by the concentration of the polymer in acetone solution that was added to water. As shown in Fig. 2 for the PSMA-based latexes, the particle size increased with increasing the polymer concentration in the acetone solution. The minimal (average) size of the latex particles was 60 nm for the latex obtained from a very dilute PSMA solution in acetone (0.01 g/ml), increasing to ~200 nm for a concentration up to 0.10 g/ml (Fig. 2). When concentrations of >0.20 g/ml were used, aggregation was observed. This phenomenon was more pronounced at higher concentrations. To obtain stable PSMA-based latexes without any aggregates, the polymer acetone solution was kept at 0.07 g/ml, giving rise to particles of ~140 nm in diameter, which was in good agreement with the cryo-TEM results reported previously [3].

The PSMA-based latex particles were found to be stabilized by electrostatic interactions [3], as a result of the ring opening of the anhydride units in the polymer by NH_3. The ζ-potential of the as-prepared latex (pH = 7) was determined to be −74 ± 2 mV, and was found to remain constant during a period of over two years. Also, the particle diameter (~140 nm) and the polydispersity index (0.12) of the particle size did not change during this period. Evidently, the particles were sufficiently stabilized by electrostatic interactions, and no additional surfactants or stabilizers were needed to obtain stable latexes.

Table 1
Polymers that were used for the preparation of different latexes

Polymer	M_n[a] (g/mol)	T_g[b] (°C)
PSMA	~5000	130
POMA	30,000–50,000	~90–100
PBDMA	5500	−70

[a] Data submitted by supplier.
[b] As determined with DSC.

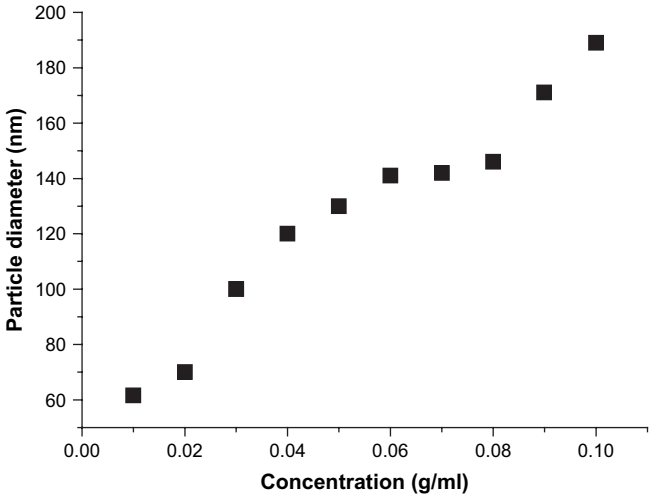

Fig. 2. Particle diameter as a function of the concentration of PSMA in acetone solution from which the latex was prepared. The polymers had 30 mol% of the anhydrides imidized with *n*-heptylamine, while another 30 mol% was ammonolyzed with NH_3 (aq., 25 wt%).

3.1.2. Latexes from other anhydride-containing polymers

In a similar way, latexes of other anhydride-containing polymers were prepared by dropwise adding the polymer solution in acetone to water. The average particle size of these latexes was about 100–200 nm, as shown in Fig. 3. Furthermore, the particles were found to have ζ-potentials in the range of −70 to −85 mV, indicating strong electrostatic stabilization of these latexes. The negative ζ-potentials can be explained by the negative charge on the amic acid moieties in the polymer backbone, since at the pH of the

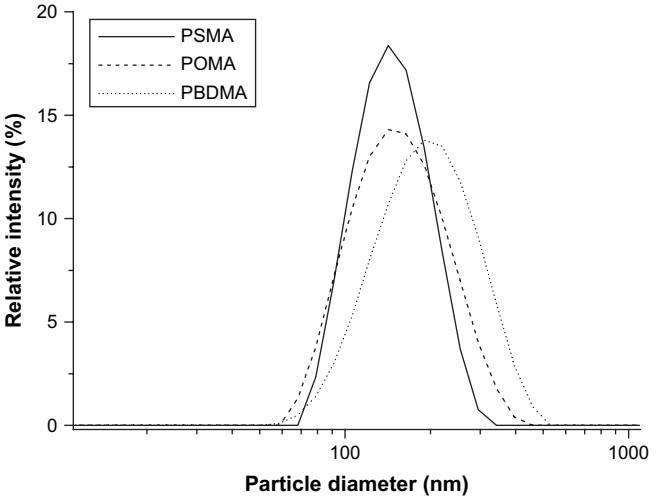

Fig. 3. Particle size distribution of latexes prepared from different polymers. The concentration of polymer in acetone added to the water phase was different for different polymer systems, i.e. 0.07 g/ml for PSMA, 0.04 g/ml for POMA, and 0.10 g/ml for PBDMA.

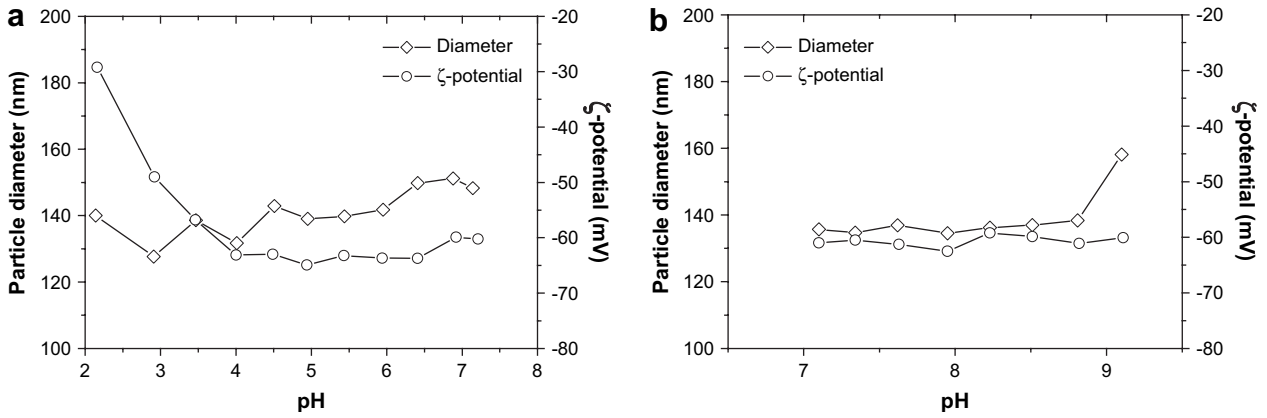

Fig. 4. pH dependence of particle size and ζ-potential of a PSMA-based latex (30 mol% of the initial anhydride was ammonolyzed and another 30 mol% was imidized with *n*-heptylamine): (a) titration with HNO_3 and (b) titration with NaOH.

as-prepared latex the H-atoms of the acid are dissociated, as indicated by the dissociation constants of the hydrolyzed polymers without ammonolysis ($pK_{a1} = 3.0$ and $pK_{a2} = 6.3$ for hydrolyzed PSMA; $pK_{a1} = 3.7$ and $pK_{a2} = 6.8$ for hydrolyzed POMA [19]). The solid contents of the artificial latexes prepared in this work were in the range of 10–15 wt%, but stable latexes up to 35 wt% solid content can be obtained.

3.1.3. Latex stability as a function of pH

3.1.3.1. PSMA-based latexes. To study the electrostatic interactions between these particles as a function of pH, DLS measurements were performed after stepwise addition of a 0.071 M HNO_3 or 0.1 M NaOH aqueous solution, directly followed by ζ-potential measurements. The measurements were performed on the latex as prepared, without the use of an electrolyte. As the pH was lowered from 7 to 2, the particle size was found to remain in the range of 130–150 nm despite the sharp ζ-potential change in the pH range of 2–4 (Fig. 4a). The ζ-potential remained relatively constant for pH values between 4 and 7, and decreased (absolute value, the same below) when the pH was lowered to below 4 (at pH = 4, a significant amount of carboxylic anions would be neutralized, leading to reduced electrostatic repulsion). Nevertheless, at a ζ-potential of −35 mV (pH = 2) the electrostatic interaction was still strong enough to prevent particle aggregation.

When the titration was performed with NaOH (0.1 M), the PSMA latex remained stable up to pH of ~9.2 (Fig. 4b). At higher pH, the imides that were formed to stabilize the polymer in aqueous environment were hydrolyzed due to the increasing basicity [20,21], and therewith the polymer became fully soluble in water. The ζ-potential was not influenced by the increasing pH, as expected, since the amic acid moieties at the particle shells were already deprotonated at pH = 7.

3.1.3.2. POMA-based latexes. POMA-based latexes displayed good stability at the initial pH (the as-prepared latex), despite that the absolute value of the ζ-potential (−42 mV) was lower compared to the PSMA latex (Fig. 5). At pH values of as low as 1.5, the particles were found to be stable, even though the ζ-potential was about −17 mV. Even after 24 h the latex was still stable, and no aggregates were observed. We also examined the latex stability under basic conditions. When the pH was in the range of 8–9.5 (Fig. 5), the latex was stable. At pH = 9.5 or above, the latex still appeared to be stable, but some flocculation was observed. However, the POMA polymer did not become fully dissolved in the alkali solution, which is likely due to the hydrophobic character of the long hexadecyl tails originating from the octadecene monomer. The hydrophobic hexadecyl groups, unlike the heptyl group in the case of PSMA-based latex, prevented the hydrolyzed POMA from being completely soluble in an aqueous environment.

3.2. Properties of latexes in the presence of a crosslinker

3.2.1. PSMA-based latexes

When DAH was added to different latexes, either from its aqueous solution or as a solid, a change in color was immediately observed, which is indicative of a reaction between the primary amine and anhydride [3], whereas the addition of ADH to the latexes did not lead to any color change. When an excess of DAH compared to the initial amount of anhydride was added, the polymers became fully soluble in water. This indicates that there was significant interaction and most probably even reaction between DAH and the latexes, whereas ADH did not seem to have any interaction with the latex particles in an aqueous environment.

For a PSMA-based latex to which 30 mol% of DAH relative to the initial anhydride was added, the pH value of the as-prepared latex increased from ~7 to ~8.5 (Fig. 6a), due to the basic nature of DAH. The ζ-potential at the initial pH changed from ~−70 mV without DAH (Fig. 4) to −45 mV after the DAH addition (Fig. 6a). Possible cause of this reduction will be discussed below. A similar decrease in ζ-potential was also observed for the addition of a similar amount of DAH to the POMA-based latex. The reduced stabilization resulted in particle aggregation when the pH was lowered to below 5, as can be seen by a significant increase in particle size (from

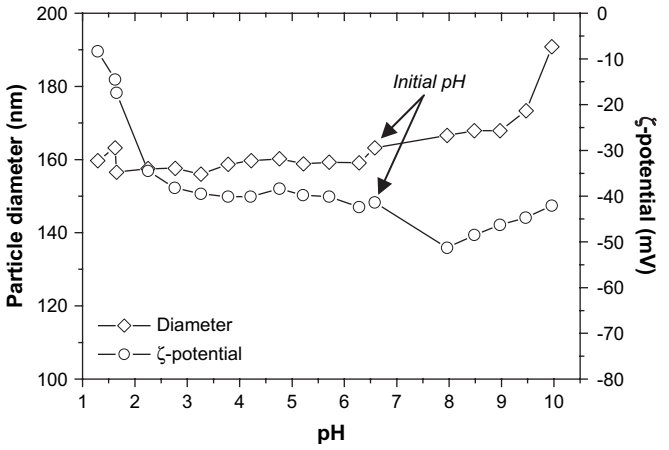

Fig. 5. pH dependence of the particle size and ζ-potential of a POMA-based latex (50 mol% of the initial anhydride was ammonolyzed).

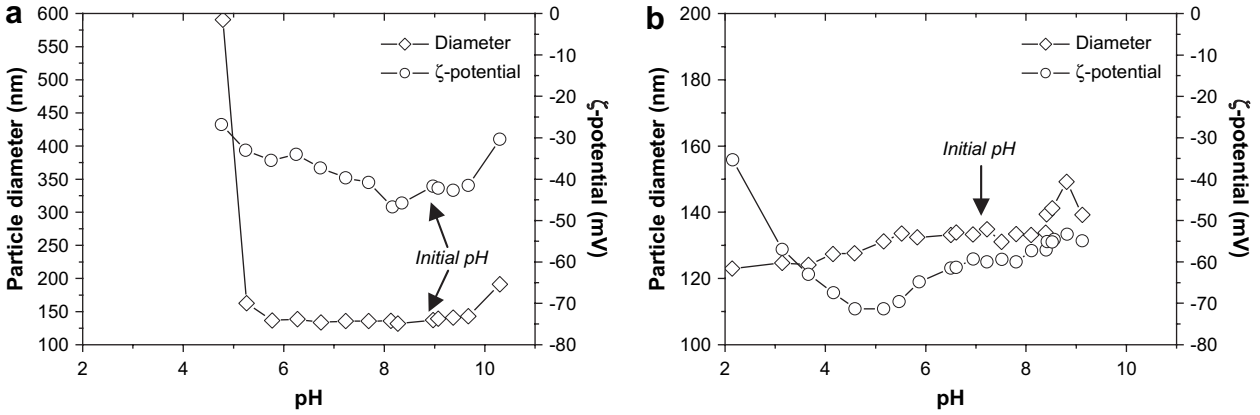

Fig. 6. pH dependence of particle diameter and ζ-potential for a PSMA-based latex at room temperature in the presence of (a) DAH and (b) ADH. Titrations were performed by adding aqueous solutions of HNO_3 to decrease or NaOH to increase the pH, starting at the initial pH of the crosslinker containing latex, as indicated by the arrows.

~150 nm to >1 μm) for the PSMA-based latex. The modulus of the ζ-potential at this pH was close to 30 mV, which is generally considered to be the value above which stable particles are obtained [22,23]. Due to the flocculation the latex with DAH could not be studied at lower pH values.

In a sharp contrast, when ADH was added to this latex, both the particle size and the ζ-potential showed similar behavior as the latex in the absence of a crosslinker, as shown in Fig. 6b. The pH of the latex as obtained was found to remain unchanged upon the addition of ADH, which indicates that the polymer particles and ADH in the aqueous phase did not interact with each other. We also examined the latex with or without ADH by cryo-TEM. The particle size and particle size distribution for the latex in the presence of ADH appeared to be similar to the latex without ADH (Fig. 7). Furthermore, no particle aggregates were observed. These results further indicate the absence of interaction between the PSMA particles and ADH in the aqueous phase.

3.2.2. POMA- and PBDMA-based latexes

For the POMA-based latex to which ADH was added, the difference between the latex with (Fig. 8) and without ADH (Fig. 5) was very small. Both the particle size and ζ-potential (Fig. 8) showed similar dependence over the whole pH range compared to the ADH-free latex. Again, at low pH values the particles were stabilized, even though the ζ-potential decreased significantly. At pH above 9.5, the particle diameter increased, indicating the onset of particle aggregates. In contrast, when DAH was added to the latex, the latex was no longer stable, leading to a gel. Due to this, no reliable pH dependence measurements for both the particle size and ζ-potential could be obtained.

For PBDMA-based latexes, a relatively high ζ-potential was found (about −80 mV), both with and without the addition of ADH. Upon the addition of DAH, however, the latex became unstable. Aggregates were observed, but the latex did not gelate like the POMA-based latex.

3.3. Interaction between crosslinker and latexes

Additional evidence for the absence of interaction between the polymers in the latexes and ADH was obtained by ^1H NMR experiments. For ADH in D_2O solution, to which sodium 3-(trimethylsilyl)propionate-d_4 (TSP) was added as a reference, two peaks (2.2 and 1.6 ppm) can be assigned to ADH. When 1 ml PSMA-based latex was added to 1 ml of this solution (50 mg/ml), the signals originating from ADH were observed at the same shifts (Fig. 9a), indicating that ADH was still dissolved in the water phase and not attached to the solid polymer particles. Since the amount of TSP added to D_2O was known, it could be used to quantify the amount of ADH that was still present in the water phase by correlating the ADH signal to the TSP signal. The TSP:ADH peak area ratio remained

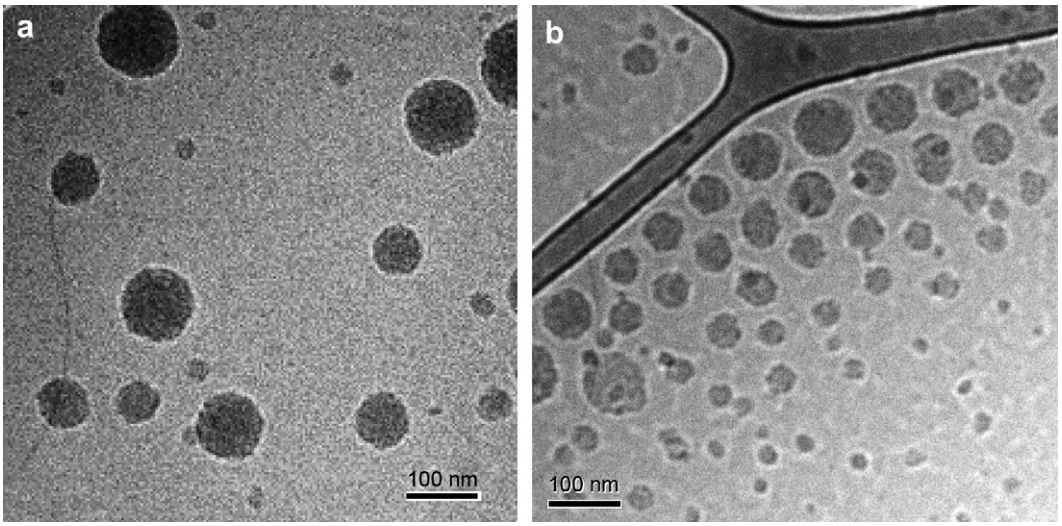

Fig. 7. Cryo-TEM pictures of a 1 wt% PSMA-based latex (a) without crosslinker and (b) with 30 mol% ADH (relative to anhydride) added.

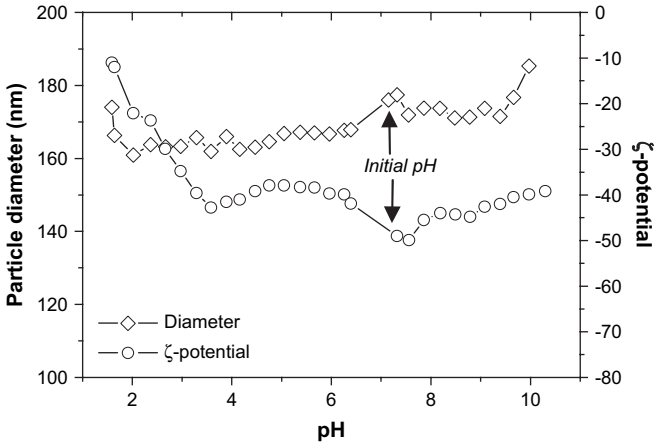

Fig. 8. pH dependence of particle diameter and ζ-potential for a POMA-based latex with ADH at room temperature.

virtually unchanged after the addition of the latex, from 1:0.90 before adding the PSMA latex to 1:0.91 after the addition of latex. This small change of the ratio was well within the experimental error and, therefore, it can be concluded that there was no interaction between latex particles and the ADH crosslinker in an aqueous environment. When the same experiment was performed with DAH, signals from unreacted DAH almost completely disappeared upon the addition of the latex (Fig. 9b). Broadened peaks (1–3 ppm) were observed, likely due to the partial dissolution of the polymer in water, which might have reacted with DAH.

To separate the crosslinker from the latexes, the mixtures were centrifuged at 60,000 rpm for 60 min. The latex in the presence of ADH did sediment under these conditions. However, the particles could be easily redispersed by shaking, and showed the same average particle size as before the centrifugation. Also the ζ-potential remained unchanged after this procedure. After the centrifugation procedure, the DAH-containing sample, on the other hand, showed some solids on the bottom, which could not be redispersed. The supernatant appeared to be yellowish, indicating the partial

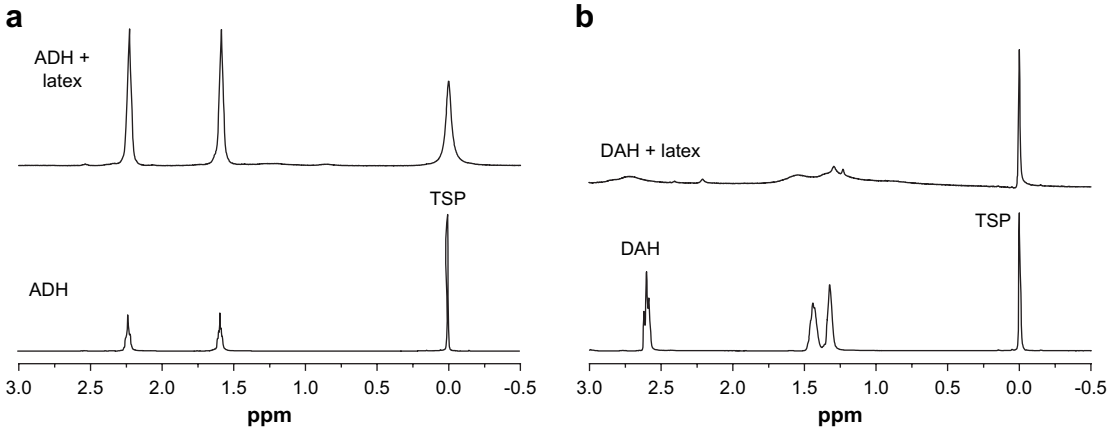

Fig. 9. (a) ^{1}H NMR spectra of ADH in D_2O (bottom) and a PSMA-based latex containing ADH (top); (b) ^{1}H NMR spectra of DAH (bottom) and a PSMA-based latex containing DAH (top). TSP was used as internal standard.

Table 2
Properties of the two crosslinkers used in this study

	ADH	DAH
Structure	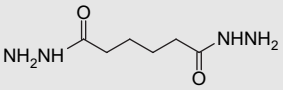	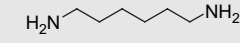
Molecular weight (g/mol)	174.2	116.2
Water solubility at 25 °C (mg/ml)	50[a]	>100[a]
pK_a	3.6 [24]	10.6 [25]
Log K_{ow}	−2.41[a]	0.02[a]

[a] Values obtained from MSDS from supplier.

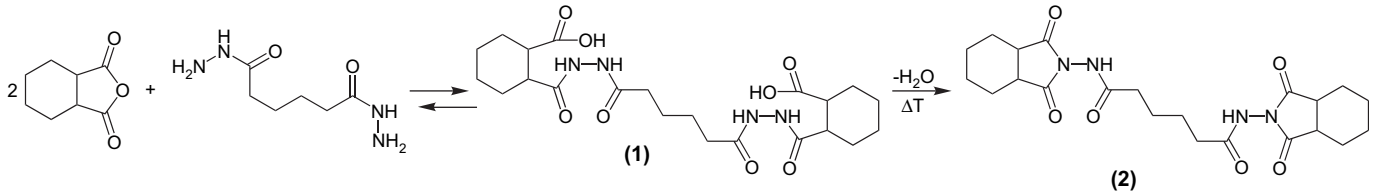

Scheme 1. Schematic representation of the reaction between CDA and ADH. The first step can take place at room temperature to yield the hydrophilic hydrazamic acid (**1**), while upon heating the ring-closed imide (**2**) is formed. Reaction between CDA and DAH follows the same route via the formation of an amic acid.

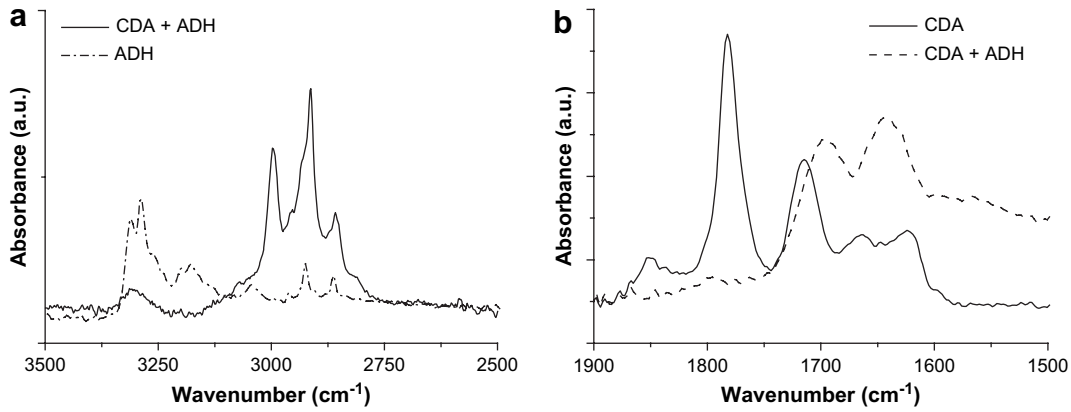

Fig. 10. ATR-FTIR spectra of the reaction product between CDA and ADH in DMSO at room temperature: (a) 3500–2500 cm^{-1} region and (b) carbonyl region. Also shown are the spectra from ADH and CDA.

dissolution of the polymer. With LC–MS, it was shown that ADH indeed was still present in the supernatant, whereas there was no signal observed originating from unreacted DAH in the corresponding system.

We further examined the possible (lack of) interaction between the two crosslinkers and the latexes by comparing the physicochemical properties of the two crosslinkers. Both compounds have reactive NH_2 groups, but their basicity and nucleophilicity differ significantly (Table 2). One major difference is that the pK_a of ADH in water is 3.6 [24], whereas the pK_a of DAH is 10.6 [25]. When the pH of the system is lower than 3.6, ADH will be protonated and be attracted by the negatively charged latex particle surface, whereas it will be in the neutral form at pH = 7. This explains the decrease of the absolute value of the ζ-potential for the ADH-latex system at pH

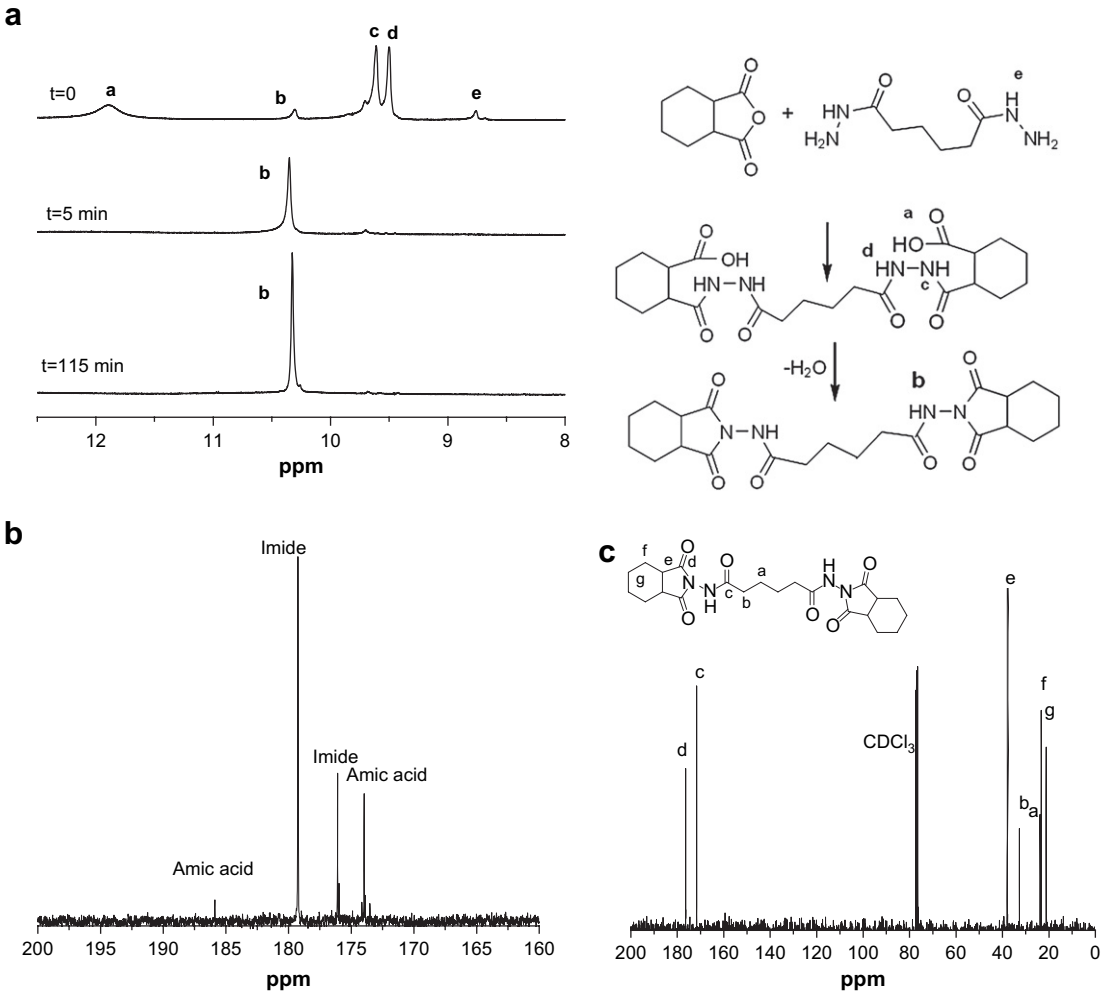

Fig. 11. (a) ^{1}H NMR spectra of the reaction mixture of CDA and ADH in DMSO-d_6 at 180 °C, and ^{13}C NMR spectra of (b) the carbonyl signals arising from the intermediate mixture of amic acid and imide during the reaction and (c) the final imide product.

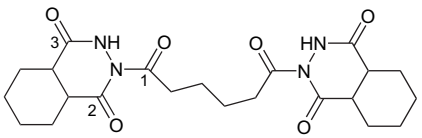

Scheme 2. The possible formation of a 6-membered ring should display three different carbonyl signals (1 ≠ 2 ≠ 3), while the 5-membered ring only displays two peaks.

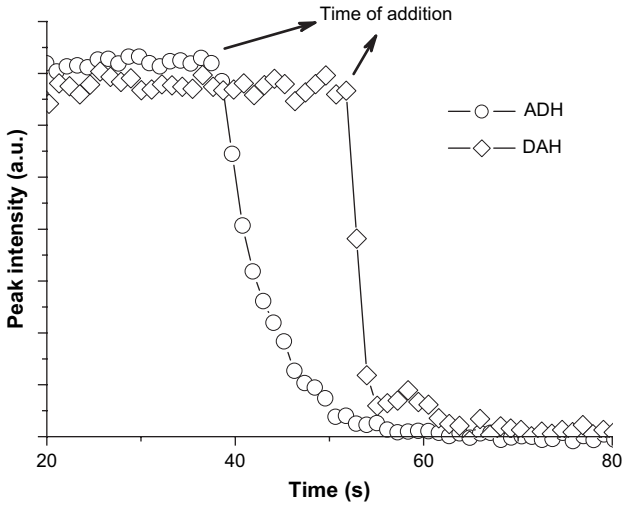

Fig. 12. Disappearance of the carbonyl signal at 1780 cm^{-1} upon mixing CDA with ADH or DAH in DMSO solutions at room temperature as a function of time, as monitored with ATR-FTIR.

values lower than 4 (Fig. 6b). The pK_a of DAH, however, is 10.6, which indicates that DAH is protonated at pH = 7 and will interact with carboxylic anions from the polymer in the latex particles, leading to the significant decrease of the absolute value of the ζ-potential (Fig. 6a), together with the absence of free DAH in the aqueous phase, as demonstrated by LC–MS analysis. Furthermore, the octanol–water partitioning coefficient, log K_{ow}, which is defined as the logarithm of the equilibrium ratio of solute concentrations in water and octanol ($K_{ow} = [solute]_{oct}/[solute]_w$) [26], of DAH is 0.02, whereas the corresponding value for ADH is −2.41. This indicates that DAH has a relative higher affinity to the lipophilic polymer particles than ADH.

On the other hand, the reactivity of ADH should be sufficient to act as a crosslinker when films are formed from the latexes. The nucleophilicity of compounds can be represented by the equation described by Patz and Mayr [27,28], who developed a general scale of nucleophilicity in different types of reactions [29]:

$$\log k = s_N(E + N) \quad (1)$$

where k is a second order rate constant (in $M^{-1}\,s^{-1}$) at 20 °C, s_N is a nucleophile-specific slope parameter, N is an electrophile-independent nucleophile-specific parameter, and E is a nucleophile-independent electrophilicity parameter [30]. Although this model has its limitations, it gives the most extensive scale of nucleophilicity presently available [29]. Since both crosslinkers will act as nucleophiles, only the N parameter was considered in this work. It is expected that the nucleophilicity for a hydrazide is comparable to that of semicarbazide [31] ($N = 11.05$, $s_N = 0.52$) [32], and therefore less nucleophilic than that of a primary amine ($N = 13.41$, $s_N = 0.65$ for *n*-propylamine) but more nucleophilic than, for instance, the nucleophilicity of aromatic amino groups [33] or ureas [34]. It is expected that this reactivity is sufficient to give crosslinked networks when mixed with anhydride-containing polymers. The nucleophilicity of DAH is estimated to be comparable to that of *n*-propylamine [30].

3.4. Model studies on crosslinking

The crosslinking process between the anhydride functional polymers and the crosslinkers used in this study consists of two steps (Scheme 1).

3.4.1. First step – ring opening

To study the crosslinking mechanism with NMR, *cis*-1,2-cyclohexanedicarboxylic anhydride (CDA) was chosen as a model compound, because PSMA showed overlapping peaks in the area of interest [35], preventing a reliable analysis. The first step of the reaction, for both ADH and DAH, consists of an addition reaction between the $-NH_2$ and anhydride groups. This reaction is known to take place at room temperature [16] (Scheme 1), to form the ring-opened amic acid (in the case of DAH), or hydrazamic acid (**1**) (in the case of ADH). For the remainder of the text the ring-opened product between anhydride and crosslinker will be referred to as amic acid.

The reaction was confirmed with ATR-FTIR. A DMSO solution containing CDA was placed on the ATR crystal, followed by adding a drop of DMSO solution containing a crosslinker. For the mixture containing equimolar amounts of anhydride and hydrazide groups, the disappearance of the anhydride signal (1780 cm^{-1}, Fig. 10b) was due to the formation of the amic acid, structure (**1**) in Scheme 1, for which carbonyl signals were found at 1640 and 1690 cm^{-1}, indicating that almost all anhydrides had reacted with ADH. In

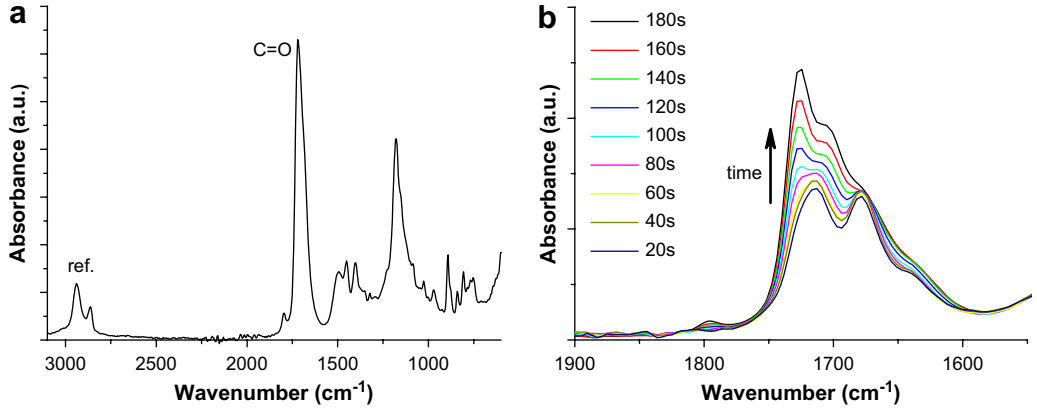

Fig. 13. (a) ATR-FTIR spectrum of the final imide product between CDA and ADH. (b) The relative intensity of the peak at 1722 cm^{-1} was monitored as a function of time at 116 °C.

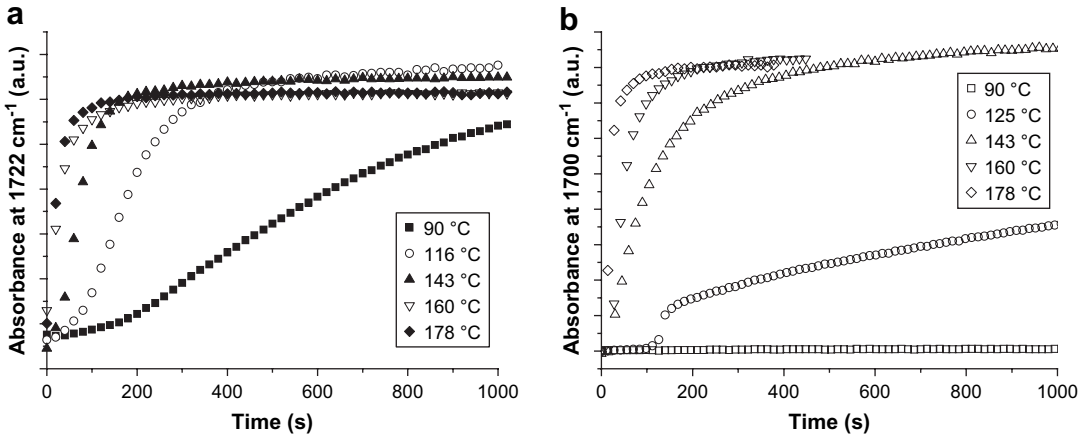

Fig. 14. Imide formation in the reaction between CDA and (a) ADH and (b) DAH, as a function of temperature by monitoring the imide carbonyl peak height.

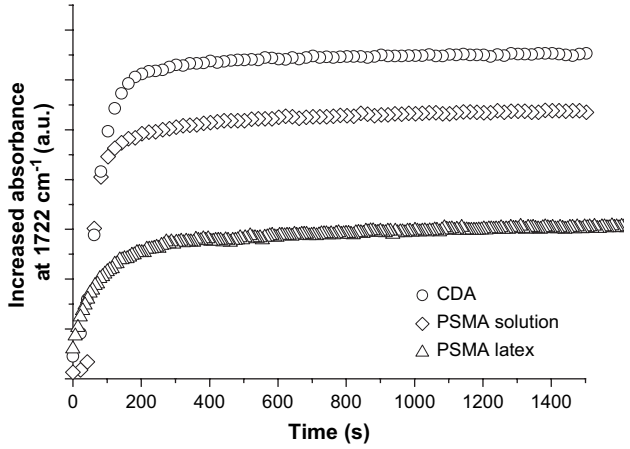

Fig. 15. Height of the carbonyl peak at 1722 cm^{-1} from the imide formed between ADH and CDA, a PSMA solution in DMSO, or a PSMA-based latex at 140 °C. The increased absorbance at time t was defined as the difference between the absorbance at time t and the initial absorbance, normalized with an internal standard.

addition, the amine signal of the free ADH (around 3300 cm^{-1}) had decreased substantially in the mixture (Fig. 10a).

3.4.2. Second step – ring closure

Ring closure of an amic acid takes place at elevated temperatures. This process was followed by ^1H NMR for a mixture of CDA and ADH in a 2:1 molar ratio. The first spectrum was immediately taken after the addition of ADH to the CDA solution at 180 °C. From the peaks arising from the amic acid (Fig. 11a) it was confirmed that the reaction between ADH and CDA took place instantaneously. Upon addition of ADH to the CDA solution, at $t = 0$, most of the two compounds immediately reacted to form the ring-opened amic acid (9.3–9.5 ppm for the amide and 12 ppm for the acid), showing only a minor peak of the unreacted ADH at 8.7 ppm. Furthermore, it was obvious that, from the appearance of a peak at 10.3 ppm at $t = 0$, the ring closure to imide took place as well. After 5 min the reaction was nearly complete at 180 °C (Fig. 11a).

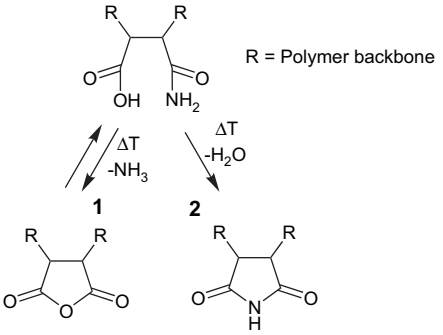

Scheme 3. The two possible ring closure options for the amic acid moiety originating from ammonolysis.

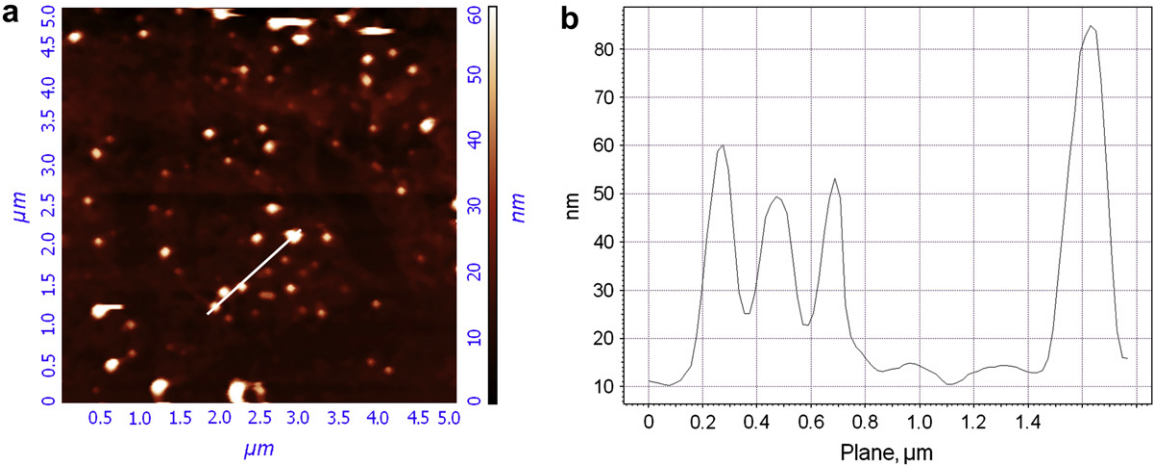

Fig. 16. (a) Semi-contact mode AFM height image of a film from 0.1 wt% PSMA-based latex with 30 mol% ADH relative to anhydride dried at room temperature, and (b) height profile of the cross-section as indicated by the line in (a).

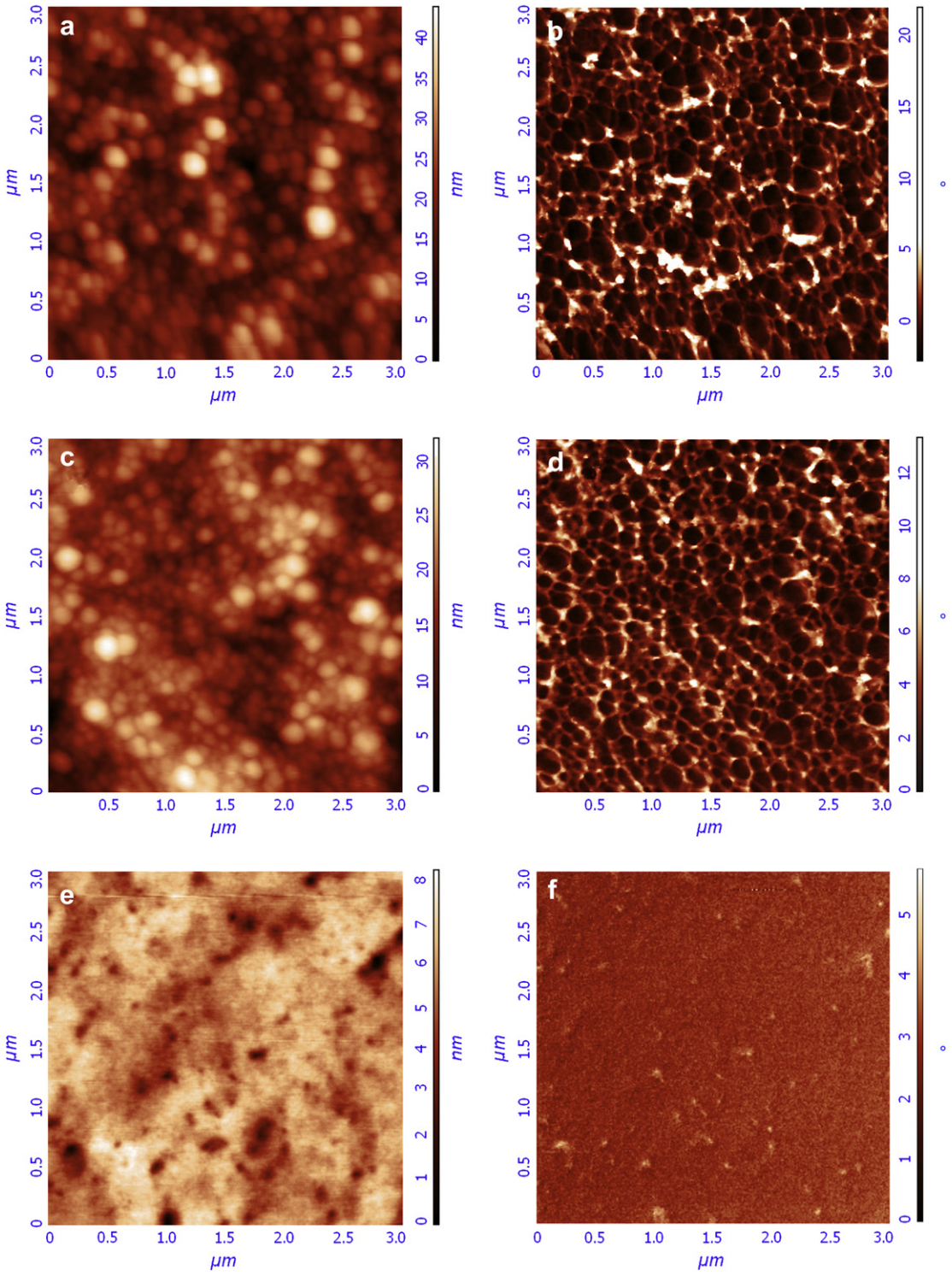

Fig. 17. Semi-contact mode AFM height (left) and phase (right) images of films from a PSMA-based latex containing 0.30 equiv ADH relative to initial anhydride, cured at ((a) and (b)) 90 °C, ((c) and (d)) 130 °C, and ((e) and (f)) 160 °C.

During the reaction, ^{13}C NMR peaks corresponding to both ring-opened amic acid and ring-closed imide were observed, as shown in Fig. 11b. The final product (**2**) of the reaction was confirmed with ^{13}C NMR without purification (Fig. 11c). Only two major peaks were found in the carbonyl region, one from the ADH (peak c) part, the other from the CDA part (peak d), indicating that only the ring-closed imide was formed under the applied reaction conditions. This also excluded the formation of a possible 6-membered ring, which would have resulted in the formation of three different signals in the carbonyl region (Scheme 2), due to the asymmetric ring structure.

The reaction between CDA and DAH was studied with ^{13}C NMR in the same way, displaying two peaks in the carbonyl region for the amic acid moiety, i.e. at 175.4 and 180.1 ppm. The final reaction product showed a single peak at 179.7 ppm, originating from the carbonyl signal of the imide. For a more detailed study on the kinetics of the crosslinking for both compounds, ATR-FTIR experiments were performed.

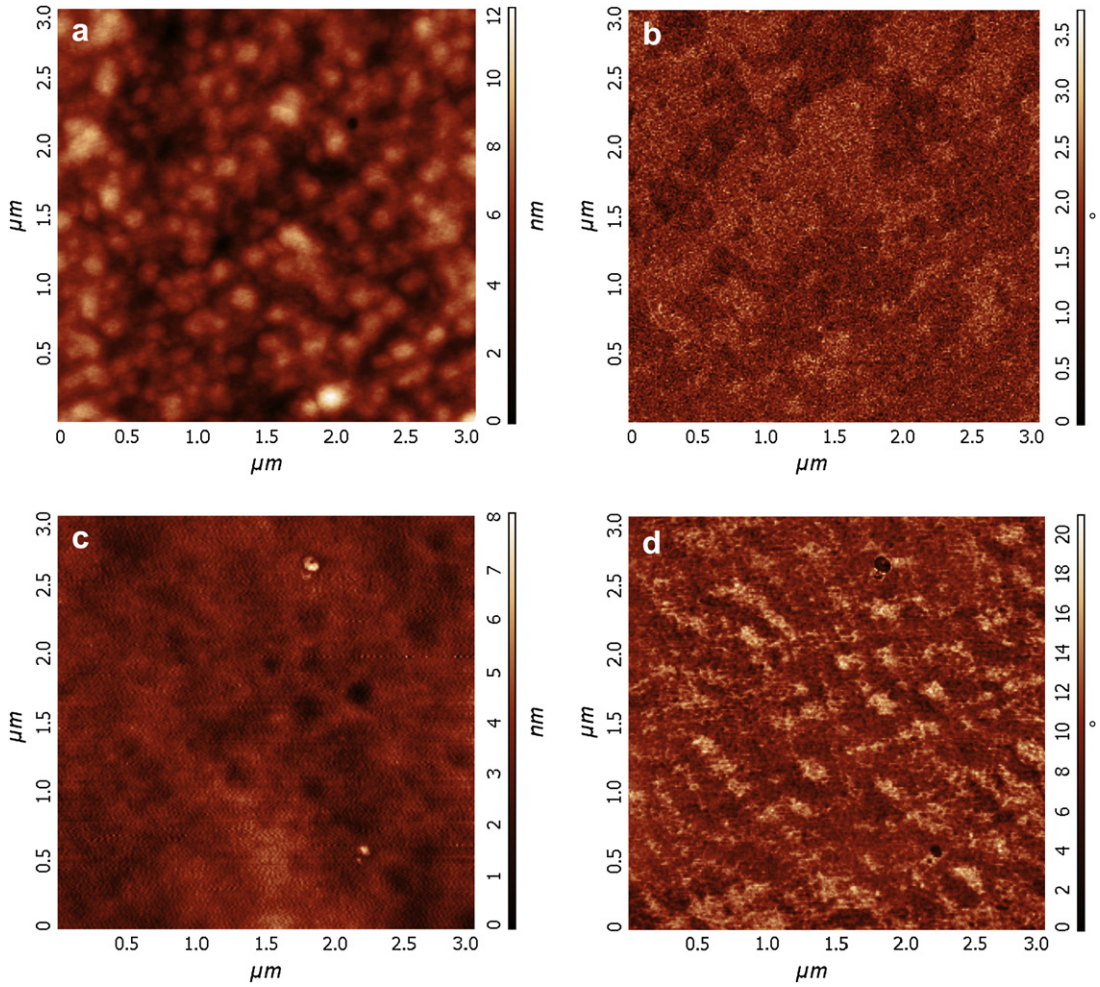

Fig. 18. Semi-contact mode AFM height (left) and phase (right) images of films from a PSMA-based latex containing 0.30 equiv of DAH relative to initial anhydride, cured at ((a) and (b)) 130 °C and ((c) and (d)) 160 °C.

3.5. Crosslinking kinetics

The first step of the crosslinking reaction was studied for CDA with DAH and ADH at room temperature in DMSO solution. Both model reactions and reactions with copolymer solutions or latexes to study the second step of the crosslinking reaction were performed at different temperatures, ranging from 90 to 180 °C.

3.5.1. Model compounds

The first step in the crosslinking was studied by following the carbonyl signal originating from the anhydride at 1780 cm^{-1}. When the decrease of the anhydride signal was followed in time, it can be seen that for ADH the time needed for the signal to have reduced to zero was longer than for DAH (Fig. 12). This confirms the more nucleophilic behavior of DAH, as indicated by the s_N and N parameters (Table 2), compared to ADH in the first step of the crosslinking reactions. ADH, however, is still reactive enough to react with anhydride and form amic acid at room temperature. The amic acid group is very hydrophilic and the reaction is reversible in an aqueous environment [12]. Therefore, a second step of heating has to be performed to obtain irreversible imide. The amic acid formed during the first step showed two peaks in the IR spectrum from the two different carbonyl groups, which both gradually disappeared upon the formation of the ring-closed imides at elevated temperatures (Fig. 13b).

The reaction between ADH and CDA was studied with ATR-FTIR by monitoring the signal at 1722 cm^{-1} (Fig. 13a), which arises from the imide carbonyl. The height of the 1722 cm^{-1} peak increased as the reaction proceeded. By following the increase of the 1722 cm^{-1} peak, with the peak at 2860 cm^{-1} of the C–H stretch signal as an internal standard, we can obtain kinetic information on the imide formation via the ring closure of the amic acid, as given in Fig. 14a. The formation of imide at 116 °C appeared to be completed within 300 s, and the reaction proceeded even faster at higher temperatures.

In a similar way, the reaction between CDA and DAH was studied (Fig. 14b). The signal arising from the imide carbonyl was found at 1700 cm^{-1}. At 90 °C, no ring closure to imide took place, contrary to the CDA/ADH system. The reaction proceeded at 125 °C, but was much slower than the CDA/ADH reaction at 116 °C. This shows that, although the formation of amic acid was faster for DAH due to its more nucleophilic nature, the second step reaction, in which the actual irreversible crosslinking would take place, was faster for ADH. As expected, the reaction proceeded faster at higher temperatures (Fig. 14b). At temperatures from 90 to 120 °C, there was some initial retardation for both ADH and DAH. This might be caused by the slow evaporation of DMSO that was used as the solvent. At higher temperatures, this retardation disappeared.

3.5.2. Polymer systems

The model reaction between CDA and ADH was compared with a PSMA solution in DMSO. The peak at 700 cm^{-1} from the phenyl ring of the styrene unit in the copolymer was used as an internal

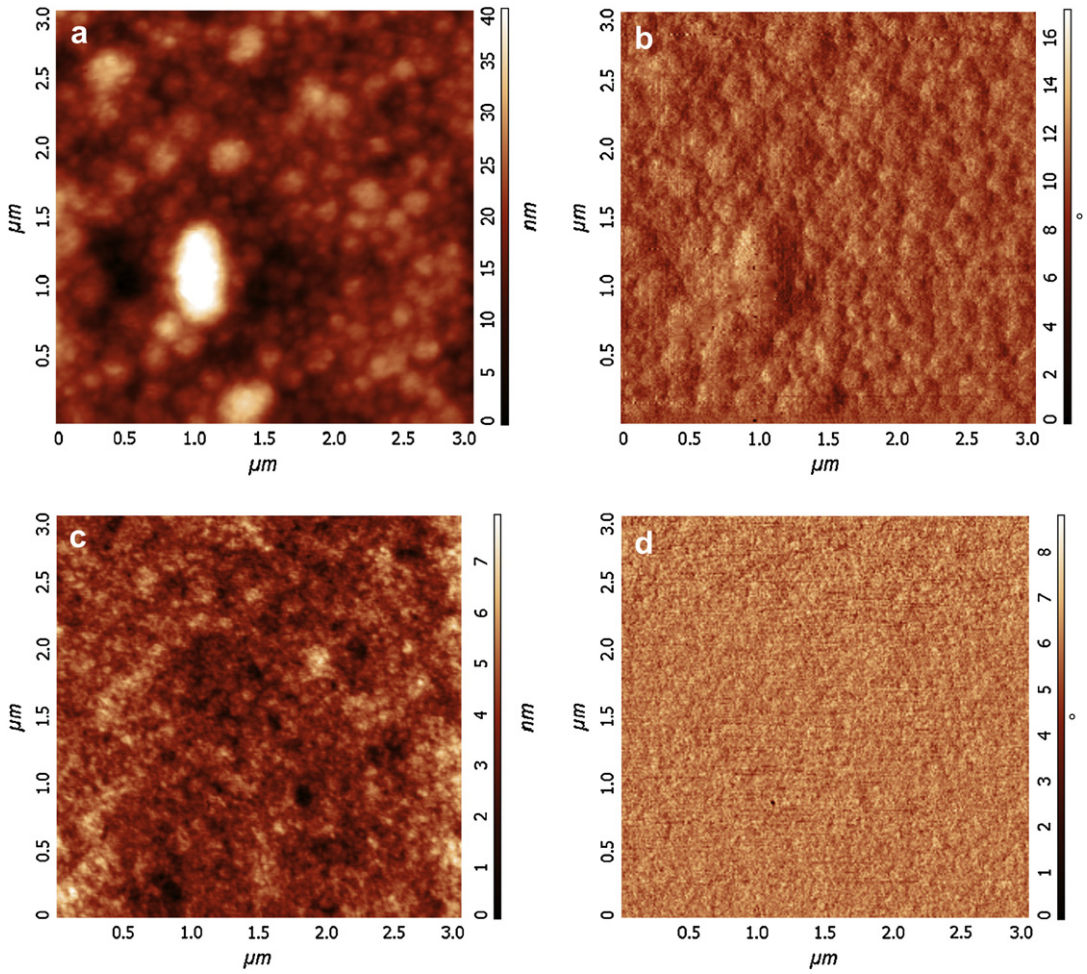

Fig. 19. Semi-contact mode AFM height (left) and phase (right) images of films from a POMA-based latex containing 0.25 equiv of ADH relative to initial anhydride, cured at ((a) and (b)) 60 °C and ((c) and (d)) 100 °C.

reference. It was found that the time to reach the plateau value for the peak height at 1722 cm^{-1} was comparable for CDA and PSMA solutions (Fig. 15). For the PSMA-based latex, a much lower plateau value for the 1722 cm^{-1} peak height was observed, which was due to the partial imidization of the initial anhydride by heptylamine in order to stabilize the latex. Nonetheless, the data in Fig. 15 indicate that the rate of reaction was comparable for the three different systems. When the ring closure reaction of the amic acid formed between DAH and the polymer or CDA was studied, the results were comparable to each other, indicating that the model compound was indeed a good model for the polymer system.

3.6. Fate of the amic acid moieties originating from ammonolysis

It has been shown that imides were formed via the ring closure, at elevated temperatures, of amic acids that were obtained at room temperature from the reaction between anhydrides and DAH or ADH crosslinkers. In addition, amic acid moieties were also formed by ammonolysis of the polymers, prior to the latex preparation. At higher temperatures, these amic acid moieties may undergo ring closure to either anhydride or imide, releasing ammonia or water, respectively (Scheme 3). This process was followed with ATR-FTIR at elevated temperatures (90–180 °C) for an aqueous solution of the fully ammonolyzed PSMA (SMA1000H). With the increasing temperature, the amount of the formed anhydride (path 1 in Scheme 3) increased, when compared to the amount of the formed imide (path 2 in Scheme 3). An estimated 30 mol% of amic acid reacted back to anhydride at 160 °C from FTIR. The amount of anhydride in the final coating should be limited, since these groups are susceptible to hydrolysis [36]. The amount of anhydride that will be present in the final coating can be limited by relatively lowering the curing temperature, and by using a higher degree of imidization or a higher amount of crosslinker. This will in turn also affect the final properties of the coatings, but the optimization of the amount of anhydride is not within the scope of this work.

3.7. Film formation

3.7.1. Films from PSMA-based latexes

3.7.1.1. Film formation at room temperature. When the films from a diluted PSMA-based latex (ca. 1 wt%), containing ADH, were dried at room temperature, no homogeneous film was obtained. Instead, individual particles with a diameter of 150–200 nm were observed (Fig. 16). This is in agreement with the particle size found with DLS and TEM. Deformation of the particles did not take place due to the relatively low temperature, which was well below the T_g of the polymer (130 °C). When this sample was heated to 150 °C, the particles did not flow, indicating that intraparticle crosslinking via the amic acid already took place prior to the deformation of the particle. Therefore, the films described in the following part were cured directly after application.

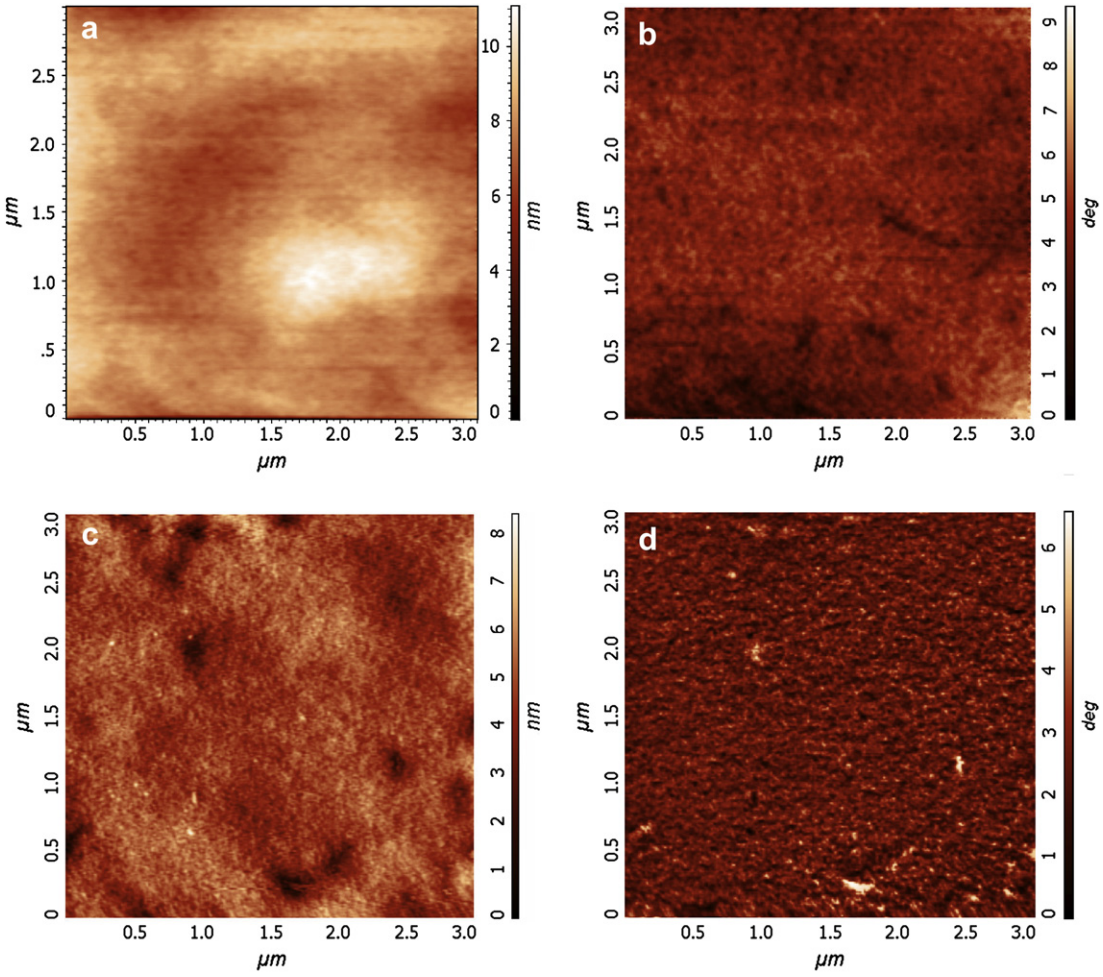

Fig. 20. Semi-contact mode AFM height (left) and phase (right) images of films from a PBDMA-based latex containing 0.25 equiv of ADH relative to initial anhydride at room temperature ((a) and (b)) and at 120 °C ((c) and (d)).

3.7.1.2. PSMA latexes crosslinked with ADH. When the film formation of a PSMA-based latex, in the presence of ADH, was performed at 90 °C, the formed films showed a rough surface (Fig. 17a), with the height variation in the range of 20–30 nm and the particle size comparable to the individual particles, indicating that the particle coalescence did not take place. Individual particles, packed but not coalesced, were also discernible in the phase image (Fig. 17b). Films cured at 130 °C showed slightly decreased surface roughness (Fig. 17c), but both height and phase images still demonstrated the particulate characteristics due to insufficient film formation. Increasing the curing temperature to 160 °C resulted in a film with the surface roughness of merely 3–5 nm (Fig. 17e), indicating that a highly crosslinked, smooth film was obtained. The very low phase contrast in Fig. 17f also confirmed the film homogeneity.

The above results suggest that a curing temperature of 160 °C was high enough to deform the particles, which is in accordance with the T_g of 130 °C of the copolymer. From the ATR-FTIR experiments it is clear that this temperature was high enough for the completion of the crosslinking, and yet not too high to cause the particles to shell-crosslink before the particle flow takes place. Increasing the curing temperature to 180 and 200 °C led to films with similar properties. A curing temperature of >200 °C would lead to the degradation of the polymers due to decarboxylation [37,38], and was therefore not studied. Furthermore, as was shown with ATR-FTIR, higher temperatures would lead to increased formation of anhydrides after ring closure of the amic acids that were obtained for the latex stabilization.

3.7.1.3. PSMA latexes crosslinked with DAH. Films of PSMA-based latexes cured with DAH at 130 °C showed more homogeneous height and phase images (Fig. 18a and b) than those cured with ADH. This might be due to incomplete crosslinking at 130 °C, yielding only the amic acid and therewith giving the polymer some freedom to move after film formation. Another cause may be the partial dissolution of the polymer due to the DAH addition, filling up the initial spaces between particles, leading to a smoother and more homogeneous image. When the curing with DAH was performed at 160 °C the phase contrast increased (Fig. 18d), despite the height variation was small (Fig. 18c), indicative of inhomogeneous crosslinking.

3.7.2. Films from POMA-based latexes

When a POMA-based latex with ADH was studied, the particle deformation should take place at lower temperatures, due to the lower T_g (~90 °C) of the polymer. As shown in Fig. 19, at 60 °C homogeneous film formation did not take place and particles of 100–200 nm were visible in both height and phase images (Fig. 19a and b), due to poor particle deformation at this temperature. Increasing the curing temperature to 100 °C, i.e. above the T_g of the polymer, led to a more homogeneous film (Fig. 19c and d). The

homogeneous film formation indicates that the ADH crosslinker was able to diffuse into the particles before the final film formation took place.

3.7.3. Films from PBDMA-based latexes

When the film formation of latexes based on PBDMA ($T_g = -72\,^{\circ}C$) was studied, homogeneous films were already obtained at room temperature (Fig. 20a and b). Also, films formed at 120 °C were homogeneous, as illustrated in both height and phase images (Fig. 20c and d). However, our ATR-FTIR data showed that no imide was formed for this system at room temperature. This was further corroborated by the very poor chemical resistance of this film, compared to the corresponding films formed at 80 °C or higher and crosslinked with ADH. At a curing temperature of 80 °C, the PBDMA-based films demonstrated excellent chemical resistance due to the formation of imide linkages.

4. Conclusions

Stable, surfactant-free artificial latexes have been successfully obtained from different anhydride-containing copolymers. The polymer particles, stabilized by electrostatic interactions after partial ring opening of the anhydride moiety by ammonia, were in the range of 100–200 nm in diameter. When a primary amine crosslinker (i.e. DAH) was added to these latexes, reactions between the particles and the amine took place immediately, leading to reduced electrostatic stabilization for the particles. In a sharp contrast, when a hydrazide based crosslinker (i.e. ADH) was added to the latex, no interaction between crosslinker and particles was observed and, thus, the addition of ADH did not affect the latex stability. This has been explained by the difference of the pK_a values between the two crosslinkers. It was found that irreversible crosslinking reactions occurred between anhydride and ADH at lower temperatures (>90 °C) than for anhydrides and DAH (>130 °C). The homogeneous film formation of the polymer latexes was related to the T_g of the copolymers and, thus, can be tuned by using copolymers with varying T_gs. ADH has been shown to be an excellent water-soluble crosslinker for the artificial latexes. These latexes based on anhydride-containing copolymers, in combination with a hydrazide crosslinker, are promising systems for water-borne coating applications.

Acknowledgements

This work was supported by Senter-Novem IOP in The Netherlands (project IOT03001). The authors thank Dirk-Jan Voorn for cryo-TEM measurements, Marion van Straten for LC–MS analyses, and Denis Ovchinnikov for his assistance in AFM measurements. Prof. H. Mayr (Ludwig-Maximilians-Universität München) is acknowledged for information on ADH reactivity.

References

[1] Doeren K, Freitag W, Stoye D. Water-borne coatings: the environmentally-friendly alternative. Munich: Hanser; 1994.
[2] Tracton AA. Coatings technology handbook. 3rd ed. London: Taylor & Francis; 2006.
[3] Soer WJ, Ming W, Klumperman B, Koning CE, van Benthem RATM. Polymer 2006;47:7621.
[4] Okude Y, Ishikura S. Prog Org Coat 1995;26:197.
[5] Teng GH, Soucek MD. J Polym Sci Part A Polym Chem 2002;40:4256.
[6] Taylor JW, Winnik MA. JCT Res 2004;1:163.
[7] Aoyagi J, Shinohara I. J Appl Polym Sci 1972;16:449.
[8] Tai H, Wang W, Howdle SM. Macromolecules 2005;38:1542.
[9] Colbeaux A, Fenouillot F, Gerard JF, Taha M, Wautier H. Polym Int 2005;54:692.
[10] Sun CX, van der Mee MAJ, Goossens JGP, van Duin M. Macromolecules 2006;39:3441.
[11] Nakayama Y. Prog Org Coat 2004;51:280.
[12] Gulbins E, Ley G. Patent US 4,894,261; 1990.
[13] Helmer BJ, Murray DL, Foster CH. Patent US 6,262,169; 2001.
[14] Kuhlkamp A, Zimmermann JW, Butschli L. Patent WO 3,345,336; 1967.
[15] Bruice PY. Organic chemistry. 2nd ed. New Jersey: Prentice Hall; 1998.
[16] Dolzhenko AV, Koz'minykh VO, Kolotova NV, Syropyatov BY, Novoselova GN. Pharm Chem J 2003;37:229.
[17] Hoffman RE, Davies DB. Magn Reson Chem 1988;26:523.
[18] Soer WJ, Ming W, Koning CE, van Benthem RATM. Prog Org Coat 2008;61:224.
[19] Osaki T, Werner C. Langmuir 2003;19:5787.
[20] Gregory JD. J Am Chem Soc 1955;77:3922.
[21] Khan MN, Khan AA. J Org Chem 1975;40:1793.
[22] Desroches MJ, Castillo IA, Munz RJ. Part Part Syst Char 2005;22:310.
[23] Hunter RJ. Introduction to modern colloid science. Oxford: Oxford University Press; 1993.
[24] Afanas'eva GV, Bychkova TI, Shtyrlin VG, Shakirova AR, Zakharov AV. Russ J Gen Chem 2006;76:757.
[25] Hall HK. J Am Chem Soc 1957;79:5441.
[26] Sangster J. Octanol–water partition coefficients: fundamentals and physical chemistry. Wiley; 1997.
[27] Mayr H, Patz M. Angew Chem Int Ed 1994;33:938.
[28] Mayr H, Kempf B, Ofial AR. Acc Chem Res 2003;36:66.
[29] Phan TB, Breugst M, Mayr H. Angew Chem Int Ed 2006;45:3869.
[30] Brotzel F, Chu YC, Mayr H. J Org Chem 2007;72:3679.
[31] Mayr H. Personal communication.
[32] Minegishi S, Mayr H. J Am Chem Soc 2003;125:286.
[33] Preston J, Ciferri A, Novi M. Acta Polym 1999;50:165.
[34] Carraher Jr CE, Burger DR. Makromol Chem 1971;142:93.
[35] Feng XS, Pan CY. Macromolecules 2002;35:4888.
[36] Rim PB, O'Connor KM. J Appl Polym Sci 1986;32:4679.
[37] Suwier DR. Flexibilised styrene-*N*-substituted maleimide copolymers with enhanced entanglement density. PhD thesis, Eindhoven University of Technology; 2001.
[38] Olea AF, Barraza RG, Fuentes I, Acevedo B, Martinez F. Macromolecules 2002;35:1049.